Determination of Rate and Equilibrium Binding Constants for Macromolecular Interactions Using Surface Plasmon Resonance: Use of Nonlinear Least Squares Analysis Methods

Daniel J. O'Shannessy,*,1 Michael Brigham-Burke,* K. Karl Soneson,† Preston Hensley,‡ and Ian Brooks‡

Departments of *Protein Biochemistry and ‡Macromolecular Sciences, SmithKline Beecham Pharmaceuticals, 709 Swedeland Road, King of Prussia, Pennsylvania 19406; and †KKS Software, Inc., 531 Westfield Dr., Exton, Pennsylvania 19341

Received December 7, 1992

Surface plasmon resonance (SPR) is a label-free, real time, optical detection method which has recently been commercialized as the BIAcore (Pharmacia). The technique relies on the immobilization of one of the interactants, the ligand, onto a dextran-coated gold surface. The second interactant, the ligate, is then injected across the surface and the interaction of the soluble ligate with the immobilized ligand is observed continuously and directly. The process of dissociation of bound ligate may also be observed directly after the sample plug has traversed the layer. Thus, the data generated contain information on the kinetic rate and equilibrium binding constants for the interaction under investigation. Historically, data from this instrument have been analyzed in terms of linear transformations of the primary data and requires that data from several ligate concentrations be analyzed to determine a single value for the association and dissociation rate constants. Here we discuss the analysis of untransformed BIAcore data by nonlinear least squares methods. The primary data are analyzed according to the integrated rate equations which describe the kinetics of the interaction of soluble ligate with immobilized ligand and the dissociation of the formed complex from the surface, respectively. Such analyses allow the direct determination of the association and dissociation rate constants for each binding experiment and, further, allow the analysis of data over a wider concentration range with lower associated errors compared to previously described methods. Through the use of modeling these interactions, we also demonstrate the limitations in determining the dissociation rate constant from the association phase of the interaction, thereby requiring that the dissociation process be analyzed. Indeed, the dissociation phase should be analyzed first to yield a relatively precise and unambiguous value of the dissociation rate constant, k_d , which can then be used to constrain the analysis of the association phase to yield a better estimate of the association rate constant, k_a . We further demonstrate that, at least for the interaction investigated, the apparent rate and equilibrium binding constants determined using SPR are concentration independent and can be determined with good reproducibility.

4. 1993 Academic Press, Inc.

The characterization of the kinetics and thermodynamics of macromolecular interactions is increasingly important for developing an understanding of the molecular basis of such events as cell adhesion and viral infection and may ultimately aid in the rational design of antagonists of such interactions. Surface plasmon resonance (SPR)² detectors, such as the BIAcore (Pharmacia), allow for the direct visualization of these macromo-

¹ To whom correspondence should be addressed. Fax: (215) 270-7359.

 $^{^2}$ Abbreviations used: SPR, surface plasmon resonance; NHS, N-hydroxysuccinimide; sCD4, recombinant, soluble form of the T-cell receptor CD4; MoAb, monoclonal antibody; EDC, N-ethyl-N'-(3-diethylaminopropyl)-carbodiimide; k_a , association rate constant; k_d , dissociation rate constant; K_D , equilibrium dissociation constant; C, ligate concentration; R, response from the SPR detector; R_{\max} , maximum response from the SPR detector; R_i , response at the point of injection of ligate, accounting for changes due to the ligate solution per se, in the absence of binding; $R_{l\rightarrow\infty}$, response after complete dissociation of bound ligate, equivalent to the system baseline response; R_a , amplitude of the dissociation process; TIR, total internal reflection.

lecular interactions in real-time, and thus the data obtained contain information on the rate and equilibrium binding constants that describe the interaction being investigated. Since SPR is a relatively new detection principle, a brief description of the physics and the BIA-core instrumentation follows.

SPR is an optical phenomenon which occurs as a result of total internal reflection (TIR) of light at a metal film-liquid interface. Total internal reflection is observed in situations where light travels through an optically dense medium such as glass and is reflected back through that medium at the interface with a less optically dense medium such as buffer, provided the angle of incidence is greater than the critical angle required for the pair of optical media. Although the light is totally reflected, a component of the incident light momentum, termed the evanescent wave, penetrates a distance of the order of one wavelength into the less dense medium, in this case buffer. The evanescent wave phenomenon has been exploited to excite molecules in close proximity to a glass-liquid interface in a process termed total internal reflection fluorescence (1).

If, however, the incident light is monochromatic and plane-polarized and the interface between the media is coated with a thin (a fraction of the light wavelength) metal film, the evanescent wave will interact with free oscillating electrons, or plasmons, in the metal film surface. Therefore, when surface plasmon resonance occurs, energy from the incident light is lost to the metal film, resulting in a decrease in the reflected light intensity. The resonance phenomenon occurs only at a precisely defined angle of the incident light. This angle is dependent on the refractive index of the medium close to the metal-film surface. Changes in the refractive index of the buffer solution, to a distance of about 300 nm from the metal-film surface, will therefore alter the resonance angle. Continuous monitoring of the resonance angle allows quantitation of changes in the refractive index of the buffer solution close to the metal-film surface. The interaction of macromolecules in the buffer solution causes a change in refractive index in close proximity to the metal-film surface which translates into a change in the resonance angle which is in turn detected and quantitated by the instrument. It is worth noting that light does not pass through the detection volume (defined by the size of the illuminated area at the interface and the penetration depth of the evanescent wave) and that the optical device is on one side of the metal-film detecting changes in the refractive index in the buffer on the opposite side. An extensive treatment of the theory of SPR may be found elsewhere (2).

Pharmacia Biosensor AB (Uppsala, Sweden) has commercialized SPR technology with an instrument called BIAcore. The instrument consists of a processing unit containing the SPR detector and an integrated microfluidics cartridge that, together with the auto-

sampler, controls delivery of sample plugs into a buffer stream passing continuously across the "sensor chip" surface. The entire system is computer controlled. The sensor chip (3–5) consists of a glass substrate onto which a thin (50 nm) gold film is deposited. The gold film is derivatized with a monolayer of a long hydroxyalkyl thiol which serves both as a "barrier" to proteins and other ligands from coming into direct contact with the metal surface and as a functionalized layer for further derivatization. A 100-nm-thick layer of carboxymethyl dextran is covalently coupled to the hydroxyalkyl thiol to produce a hydrophilic surface for immobilization of macromolecules.

By continuously monitoring the refractive index (RI), detected as a change in the resonance angle, in the detected volume and plotting this value as a function of time, a sensorgram is obtained. The y-axis of the sensorgram is denoted the resonance signal and is indicated in response units (RU). A change in signal of 1000 RU corresponds to a 0.1° shift in the surface plasmon resonance angle and for globular proteins is equivalent to a surface concentration of 1 ng/mm² (6). The total range covered by the SPR detector is 3°, or 30,000 RU. The resonance signal at any given point in time is the sum of contributions from the sensor chip surface, interacting molecules, and the bulk solution (6). Under conditions of constant bulk solution refractive index, the amount of interacting molecule can be monitored continuously. If, on the other hand, the refractive index of the ligate solution differs from that of the continuous buffer flow, the amount of interacting ligate may be quantitated from readings taken between sample injections where constant RI buffer flow is operating. For kinetic measurements, where the progress of the binding curve rather than the absolute response values are used, correction for sample bulk refractive index is not necessary.

Traditionally, the analysis of BIAcore binding data for the determination of rate and equilibrium binding constants has involved linear transformations of the primary data (7-12). However, linear transforms also transform the parameter-associated errors with the result that they no longer reflect the high quality primary data obtained on the BIAcore. In addition, the linear approach to data analysis requires that data obtained from many ligate concentrations be used to derive single values for the kinetic rate and thus the equilibrium binding constant. In the present paper, however, we describe nonlinear least squares methods of analysis of the binding data obtained on the BIAcore which allow for the determination of the kinetic rate and equilibrium binding constants for each binding experiment. We further discuss the consequences of this approach on the quantitation of kinetic rate and equilibrium binding constants determined by SPR. As a model macromolecular system, we chose to study the interaction between the

soluble form of the T-cell accessory molecule CD4 (sCD4) and a mouse monoclonal antibody, L71 (13,14).

KINETIC ANALYSES—THEORETICAL ASPECTS

Since the SPR detector is a continuous, real-time detector, the possibility for assessing the kinetics of interaction exists. As noted earlier, the interaction observed is between an immobilized ligand and a soluble ligate.

For the reversible interaction,

$$A + B \stackrel{k_a}{\longleftrightarrow} AB$$

the rate of formation of the product, AB, at time t may be written as

$$d[AB]/dt = k_a[A][B] - k_d[AB],$$
[1]

where k_a is the association rate constant and k_d is the dissociation rate constant. After some reaction time, t, $[B] = [B]_0 - [AB]$. Substituting into [1] gives

$$d[AB]/dt = k_a[A]([B]_0 - [AB]) - k_d[AB],$$
 [2]

where $[B]_0$ is the concentration of B at t = 0.

In the BIAcore, one of the interactants is immobilized onto the surface and the other is continuously replenished from the injection volume flowing over the surface. The signal observed, R, is proportional to the formation of AB complexes at the surface and the maximum signal, R_{\max} , will be proportional to the surface concentration of active ligand at the surface (7). In the case of the BIAcore, therefore, Eq. [2] becomes

$$dR/dt = k_a C(R_{max} - R) - k_d R, \qquad [3]$$

where dR/dt is the rate of formation of surface associated complexes, i.e., the derivative of the observed response curve, C is the constant concentration of ligate in solution; R_{\max} is the capacity of the immobilized ligand surface expressed in resonance units, and $(R_{\max} - R)$ is equivalent to the number of unoccupied surface binding sites at time t. Note that since terms in R appear on both sides of the equation, the response value R can be used directly without conversion to absolute concentrations of formed complexes at the sensor chip surface. Rearranging [3] gives

$$dR/dt = k_a C R_{\text{max}} - (k_a C + k_d) R$$
 [4]

Traditional analyses of binding data obtained on BIAcore have utilized Eq. [4]. In such analyses a plot of dR/dt versus R yields a slope, k_s , defined as

$$k_s = k_a C + k_d. ag{5}$$

Determination of k_s at a number of ligate concentrations (C) allows one to plot k_s versus C from which a single value for k_a , the slope, and k_a , the y-intercept, is obtained. However, linear transforms, such as the one described above, also transform the errors in the primary data. This has the result that the errors in the derived parameter values no longer directly reflect the errors in the observed response (15–17). In addition, little information is obtained to define the reproducibility or certainty in the derived parameters.

For these reasons, it is advantageous to analyze data directly in terms of the integrated form of the rate equation

$$R_{t} = \frac{Ck_{a}R_{\max}[1 - e^{-((Ck_{a} + k_{d})t)}]}{Ck_{a} + k_{d}}$$
[6]

Equation [6] defines $R_{t=0}$ as zero. However, the baseline response of the instrument prior to injection of ligate is not zero. Baseline correction, or normalization, of the primary data can be achieved by subtracting the response before the injection of ligate from the response values obtained during the progress of the binding curve and fitting to Eq. [6]. While baseline correction of data is valid, the requirement is that the baseline response is precisely known.

An alternative approach to baseline correction is described by

$$R_{t} = \left\{ \frac{Ck_{a}R_{max}[1 - e^{-((Ck_{a} + k_{d})t)}]}{Ck_{a} + k_{d}} \right\} + R_{i},$$
 [7]

where R_i is an additional fitting parameter equivalent to the signal at the point of injection of ligate (t=0), which, as noted above is not zero. In addition, this parameter accounts for any change in response due to the refractive index of the soluble ligate, in the absence of binding. The untransformed primary data, i.e., R versus t, obtained from the association phase can therefore be fit directly to Eq. [7] without baseline correction. Using the integrated form of the rate equation (Eq. [7]), errors in the derived parameters, k_a and k_d , directly reflect errors in the primary data. This approach also has the additional advantage that k_a and k_d can potentially be determined for every binding experiment.

Importantly, the process of dissociation of the formed complexes, AB, can also be observed directly once the ligate solution has traversed the flow cell and the system reverts to buffer flow. The rate of dissociation of the formed complexes, AB, is described by

$$dR/dt = -k_d R. ag{8}$$

Previous reports on the analysis of the dissociation process observed using BIAcore have again used a linearized form of Eq. [8] described by

$$\ln(R_1/R_n) = k_d(t_n - t_1), [9]$$

where R_1 is the response at t=1 and R_n is the response at time t=n along the dissociation curve. Therefore, a plot of $\ln(R_1/R_n)$ versus (t_n-t_1) should produce a straight line of slope k_d . For the reasons described above, it is advantageous to analyze the dissociation process in terms of the integrated rate equation

$$R_t = R_{\mathbf{a}} e^{-k_d t}, ag{10}$$

where R_a is defined as the amplitude of the dissociation process.

To account for the fact that even after complete dissociation of the complex, AB, from the surface of the sensor chip the instrument response is not zero, Eq. [10] may be rewritten as

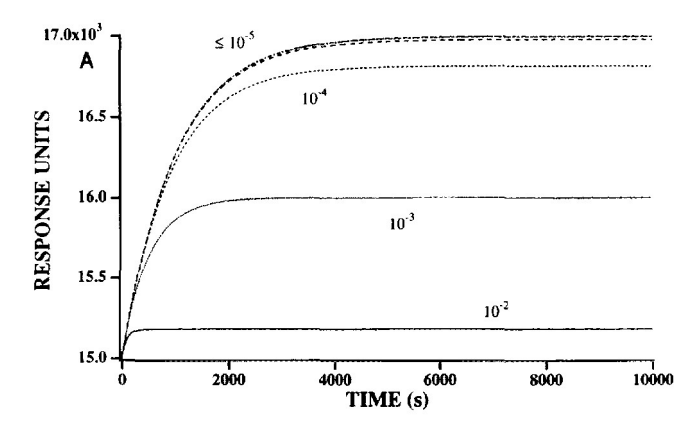
$$R_t = \{R_{\mathbf{a}}e^{-k_d t}\} + R_{(t \to \infty)}, \qquad [11]$$

where $R_{t\to\infty}$ is the response value after infinite time and represents complete dissociation of the AB complexes, and $R_{\rm a}$ is the amplitude of the dissociation process. Again, inclusion of the fitting parameter $R_{t\to\infty}$ obviates the need for baseline correction of the data set.

As described above for the analysis of the association phase (Eq. [7]), the untransformed data obtained during the dissociation process may be analyzed directly according to Eq. [11] allowing for the quantitation of the dissociation rate constant, k_d , for every binding experiment. The importance of the analysis of both the association and the dissociation phases will be discussed below.

MATERIALS AND METHODS

The BIAcore system used in these studies is manufactured by Pharmacia Biosensor AB (Uppsala, Sweden). Sensor chips CM5, surfactant P20 and the amine coupling kit containing N-hydroxysuccinimide (NHS), N-ethyl-N'-(3-diethylaminopropyl)-carbodiimide (EDC) and ethanolamine hydrochloride were from Pharmacia Biosensor AB. Recombinant human sCD4 (domains D1 through D4) and the mouse IgG1 monoclonal antibody (MoAb) L-71 were obtained from Raymond Sweet (Department of Molecular Genetics, SmithKline Beecham Pharmaceuticals). MoAb L-71 has an epitope specificity for amino acids 87 through 89 in the D1 domain (v3 loop) of CD4 (Raymond Sweet, personal communication). The recombinant human sCD4 used in the present studies was shown by analytical ultracentrifuge analysis to be a monomeric species with a molecular weight of 45 kDa (Hensley, personal communication). The graphing and data analysis program, IGOR, was purchased from WaveMetrics (Lake Oswego, OR).



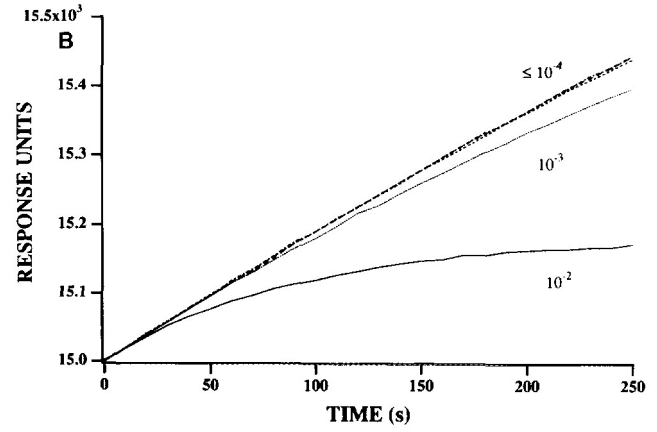


FIG. 1. Effect of k_d on the association progress curve. Equation [7] was used to generate model data sets using the following parameter values: $R_i = 15,000 \text{ RU}$, $R_{\text{max}} = 2000 \text{ RU}$, $C = 10^{-8} \text{ M}$, $k_a = 10^5 \text{ M}^{-1} \text{ s}^{-1}$, and k_d was varied from 10^{-2} s^{-1} to 0, i.e., pure association. (A) Association progress curves over a 10,000-s time period, (B) expanded view of the same curves over the initial 250 s, the time period for which BIA-core binding data are routinely obtained. Gaussian noise of $\pm 1 \text{ RU}$ was added to all model data sets to better simulate real BIAcore data.

Immobilization of MoAb L71 was performed as previously described by reaction of the ligand associated amines with an N-hydroxysuccinimide-ester activated surface (13). Briefly, after equilibration of the instrument with Hepes buffer (HBS: 10 mm Hepes, 150 mm NaCl, 0.05% surfactant P20, pH 7.4), the following sample injections were made using the automated robotics unit incorporated into the BIAcore instrument: (i) equal volumes of NHS (0.1 M in water) and EDC (0.1 M in water) were first mixed by the robot after which 30 μ l was injected across the surface to activate the carboxymethylated dextran; (ii) ligand (30 µl, 30 µg/ml 10 mM sodium acetate, pH 4.7) was then injected across the activated surface; (iii) residual NHS-esters on the sensor chip surface were then reacted with ethanolamine (30 µl, 1 M in water, pH 8.5); (iv) noncovalently bound ligand was then washed from the surface by injecting phosphoric acid (15 µl, 0.1 M). The immobilization protocol was performed with a continuous flow of HBS of 5

10⁴ 10³

250

TABLE 1
Effect of Dissociation Rate Constant on the Association Phase

	Calculated parameter values (± % SD) ^b		
Input k_d $(s^{-1})^a$	k _a	$R_{ m max}$	k_d
1×10^{-2}	$9.96 \times 10^4 (\pm 1.73)$	1994 (±1.69)	$9.90 \times 10^{-3} \ (\pm 0.43)$
1×10^{-3}	$9.99 \times 10^4 (\pm 1.42)$	$2000 (\pm 1.33)$	$9.86 \times 10^{-4} \ (\pm 1.35)$
1×10^{-4}	$9.99 \times 10^4 (\pm 1.15)$	1999 (±1.01)	$9.82 \times 10^{-5} \ (\pm 1.74)$
1×10^{-5}	$9.50 \times 10^4 \ (\pm 1.23)$	$2101 \ (\pm 1.09)$	$4.52 \times 10^{-5} \ (\pm 2.08)$
1×10^{-6}	$1.00 \times 10^5 \ (\pm 1.14)$	1999 (±1.00)	$9.88 \times 10^{-6} \ (\pm 3.25)$
0	$9.79 \times 10^4 \ (\pm 1.19)$	$2042 \ (\pm 1.05)$	$1.06 \times 10^{-5} \ (\pm 2.70)$

^a The parameter values used to generate the data sets were as described in the legend to Fig. 1.

 μ l/min. Immobilization of ligands typically takes 30 min.

Using a single immobilized L71 surface, $40~\mu l$ of sCD4 prepared at various concentrations in HBS was injected and allowed to interact with the layer. After the injection plug had passed the surface, the dissociation process was allowed to proceed for an additional 10,000~s. The L71 surface was regenerated between sCD4 injections with $10~\mu l$ 0.1 M phosphoric acid. Phosphoric acid regeneration has previously been shown not to affect the functional capacity of immobilized L71 (13). In the present experiments, a constant flow rate of $5~\mu l/min$ was used throughout unless otherwise noted and data were collected at 1 Hz. However, both the flow rate and the sample collection rate can be varied.

Data were analyzed directly using the integrated form of the rate equations using IGOR on a Macintosh personal computer. Data from the association phase were analyzed according to Eq. [7] and the dissociation phase was analyzed according to Eq. [11]. Routines for importing and analyzing BIAcore binding data were written by the authors and encoded into IGOR. IGOR uses the Levenberg-Marquardt algorithm for iterative curve fitting (18).

RESULTS AND DISCUSSION

Modeling Studies

In the design of the BIAcore microfluidics system, the injection of ligate is limited to a maximum of 50 μ l. Therefore, data which describe the association phase of the macromolecular interaction can only be collected for a short period of time (≈ 300 s). Given this limitation, model data sets were generated, according to Eq. [7], to help define our ability to determine kinetic rate constants from the association phase of BIAcore bind-

ing data. An example of this is presented in Fig. 1A where data sets were generated using the following parameters as defined by Eq. [7]: $R_{\rm i}$ = 15000 RU, $R_{\rm max}$ = 2000 RU, $C = 10^{-8}$ M, $k_a = 10^{5}$ M⁻¹ s⁻¹, and k_d varied from 10⁻² s⁻¹ to 0, i.e., pure association. An association rate constant of 10⁵ M⁻¹ s⁻¹ was considered to be a reasonable guess for the interaction of a MoAb with its antigen, such as in the present investigation. It can be seen from Fig. 1 that even if one could continuously inject ligate for 10,000 s, it is difficult to distinguish between dissociation rate constants below 10⁻⁵ s⁻¹ in the association process. Further, and more importantly, in the time period of an association phase that is routinely observed on the BIAcore run according to the manufacturer's recommendations, dissociation rates below 10⁻⁴ s⁻¹ cannot be distinguished from pure association, i.e., a dissociation rate of 0 (Fig. 1B). To further demonstrate this point, the model data sets presented in Fig. 1B were fit to Eq. [7] and the calculated parameter values are pre-

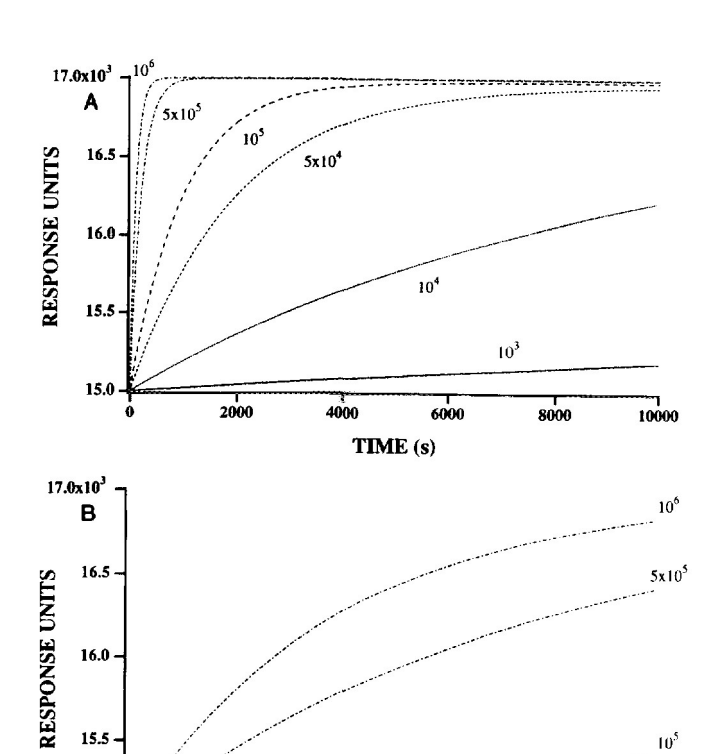


FIG. 2. Effect of k_a on the association progress curve. Equation [7] was used to generate model data sets using the following parameter values: $R_i = 15,000 \; \mathrm{RU}$, $R_{\mathrm{max}} = 2000 \; \mathrm{RU}$, $C = 10^{-8} \; \mathrm{M}$, $k_d = 10^{-5} \; \mathrm{s}^{-1}$, and k_a varied from $10^3 \; \mathrm{to} \; 10^6 \; \mathrm{M}^{-1} \; \mathrm{s}^{-1}$. (A) Association progress curves over a 10,000-s time period, (B) expanded view of the same curves over the initial 250 s, the time period for which BIAcore binding data are routinely obtained. Gaussian noise of $\pm 1 \; \mathrm{RU}$ was added to all model data sets to better simulate real BIAcore data.

TIME (s)

100

150

200

^b Curve fitting was performed, according to Eq. [7], by floating all parameters except ligate concentration, *C. R*, was calculated to excelent precision in all instances and is therefore not presented in the table.

TABLE 2
Effect of Association Rate Constant on the Association Phase

	Calculated parameter values $(\pm \% \text{ SD})^b$		
Input $k_a (M^{-1} s^{-1})^a$	k _a	R _{max}	
$1 imes 10^3$	$5.46 \times 10^3 \ (\pm 4.69)^c$	384 (±4.54)	
1×10^4	$1.02 \times 10^4 (\pm 2.71)$	1975 (±2.67)	
$5 imes 10^4$	$4.95 \times 10^4 \ (\pm 1.68)$	$2019\ (\pm 1.58)$	
$1 imes10^{5}$	$9.96 \times 10^4 \ (\pm 0.92)$	$2007 (\pm 0.82)$	
$5 imes 10^5$	$5.00 \times 10^5 \ (\pm 0.08)$	1999 (±0.04)	
$1 imes10^6$	$1.00 \times 10^6 \ (\pm 0.04)$	2000 (±0.01)	

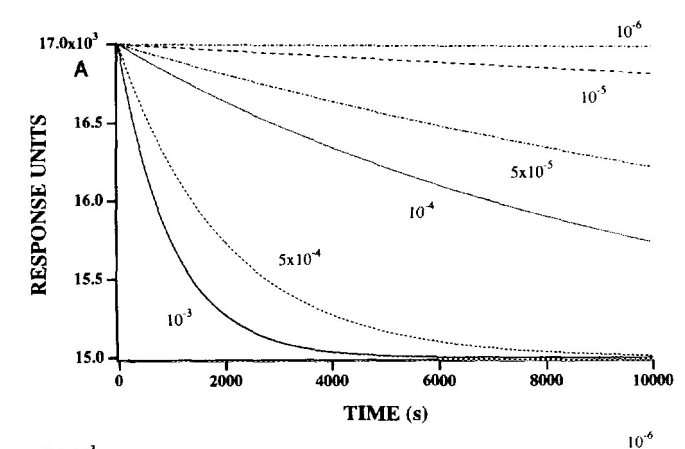
"The parameter values used to generate the data sets were as described in the legend to Fig. 2.

'If R_{max} was fixed at a value of 2000 RU, a value of 1.14 \times 10³ (±2.52%) could be determined for k_a .

sented in Table 1. While k_a , $R_{\rm max}$, and $R_{\rm i}$ can all be derived with good precision, it can be seen that a dissociation rate constant below about $10^{-4}~{\rm s}^{-1}$ cannot be distinguished from pure association.

On the other hand, for a given dissociation rate constant (10^{-5} s^{-1}) , a wide range of association rate constants can be distinguished, even over short time periods (see Fig. 2) Clearly, however, the longer the time period over which data are collected and analyzed, the greater the ability to accurately define the parameters which describe the interaction. The parameter values calculated according to Eq. [7] for the data presented in Fig. 2B are presented in Table 2. Except for the data set generated using a k_a of 10^3 M⁻¹ s⁻¹, all parameter values were calculated accurately and with good precision. The inability to derive a k_a of 10^3 M⁻¹ s⁻¹ is not unexpected given that the ligate concentration used to generate these data sets was 10^{-8} M.

The inability to inject more than 50 µl of ligate solution could thus be considered a limitation of the BIAcore in its present form. However, since injection of sample and bulk buffer flow over the sensor surface is controlled by pneumatic valves, it may be possible to reprogram the instrument to allow for larger volume injections of ligate by bypassing the sample loops entirely. Since the injection syringe, as presently configured, has a 500-µl volume, such a modification would allow for a 10-fold increase in ligate injection volume and thus a 10-fold increase in the amount of data obtained to describe the association process. Not only would this allow a better definition of the association rate constant, but the ability to derive dissociation rate constants from the association phase would be greatly enhanced (see Figs. 1 and 2). The advantage of this would be that the dissociation rate constant could be



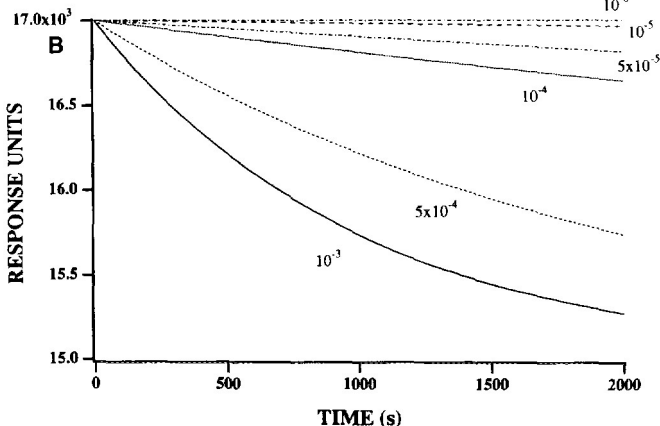


FIG. 3. Effect of k_d on the dissociation progress curve. Equation [11] was used to generate model data sets using the following parameters: $R_{t\to\infty} = 15,000 \text{ RU}$, $R_a = 2000 \text{ RU}$, and k_d varied from 10^{-3} to 10^{-6} s⁻¹. (A) Dissociation progress curves over a 10,000-s time period, (B) the same curves over the first 2000 s. Gaussian of $\pm 1 \text{ RU}$ was added to all model data sets to better simulate real BIAcore data.

determined from both the association and the dissociation phases.

In contrast to the limited time available to observe the association phase, the dissociation phase may be observed with buffer flow for an extended period of

TABLE 3

Determination of the Dissociation Rate Constant

	Calculated parameter values (± % SD) ^b		
Input k_d (s ⁻¹) ^a	k _d	R_a	$R_{t \to \infty}$
$\begin{array}{c} 1\times10^{-6} \\ 1\times10^{-5} \\ 5\times10^{-5} \\ 1\times10^{-4} \\ 5\times10^{-4} \\ 1\times10^{-3} \end{array}$	$9.96 \times 10^{-7} \ (\pm 0.90)$ $1.00 \times 10^{-5} \ (\pm 0.50)$ $4.95 \times 10^{-5} \ (\pm 0.09)$ $9.97 \times 10^{-5} \ (\pm 0.04)$ $5.00 \times 10^{-4} \ (\pm 0.01)$ $1.00 \times 10^{-3} \ (\pm 0.02)$	1988 (±1.42) 1995 (±0.40) 2015 (±0.07) 2003 (±0.03) 2000 (±0.01) 2000 (±0.01)	15,012 (±0.19) 15,005 (±0.06) 14,985 (±0.01) 14,997 (±0.0) 15,000 (±0.0) 15,000 (±0.0)

[&]quot;The parameter values used to generate the data sets were as described in the legend to Fig. 3.

^b Curve fitting was performed, according to Eq. [7], by floating all parameters except ligate concentration, C, and the dissociation constant, k_d . R_i was calculated to excellent precision in all instances and is therefore not presented in the table.

^b Curve fitting, according to Eq. [11], was performed by floating all three parameters.

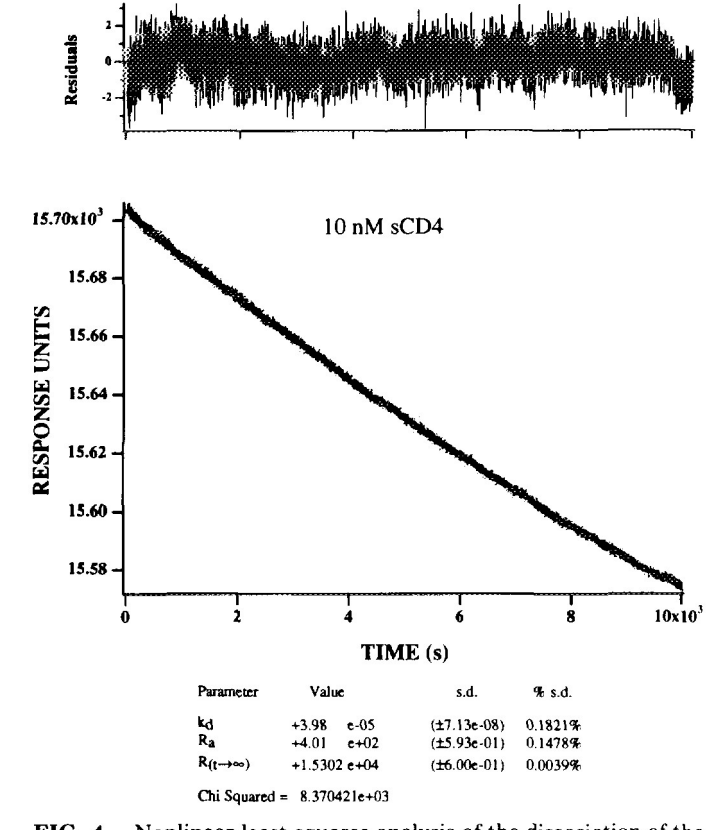


FIG. 4. Nonlinear least squares analysis of the dissociation of the sCD4-L71 complex. sCD4 at a concentration of 10 nM was injected across the immobilized L71 layer as described under Materials and Methods. After the sample plug had traversed the layer, the process of dissociation was followed for 10,000 s. The data were then analyzed according to Eq. [11] as described. The actual data points (1 per second) and the calculated line are shown on the graph. A residual plot, which is basically random with an amplitude of ± 2 RU, is also shown. The fitted parameters for this data set were: $k_d = 3.98 \times 10^{-5} \pm 7.13 \times 10^{-8} \rm s^{-1}$, $R_a = 401 \pm 1$ RU, and $R_{t\rightarrow \infty} = 15,302 \pm 1$ RU.

time. Model data sets generated according to Eq. [11] demonstrate that dissociation rate constants to as low as 10^{-6} s⁻¹ can be distinguished from one another (see Fig. 3). Table 3 demonstrates that the parameter values used to generate the data sets shown in Fig. 3 can be derived from these data sets with good accuracy. Taken together, therefore, these model data (Figs. 1-3 and Tables 1-3) suggest that the most thorough analysis of BIAcore data includes analysis of both the association and the dissociation phases of the interaction, particularly if the equilibrium binding constant for the interaction is high. Furthermore, since one's ability to extract dissociation rate constants from the association phase is dependent on the magnitude of the dissociation rate constants, we suggest that the dissociation process be analyzed first. The above described modeling studies are not presented to define the absolute limits in the magnitude of kinetic rate constants that can be determined using the BIAcore, but merely serve to illustrate the importance of analyzing both the association phase and the dissociation phase of the interaction under investigation. It is the belief of the authors that for kinetic analyses using BIAcore, the dissociation phase should be analyzed first to yield a relatively precise and unambiguous value of k_a which can then be used to constrain the analysis of the association phase to yield a better estimate of k_a .

Data Analyses

Based on the above discussion, it is clear that careful analysis of the dissociation phase is important since the magnitude of the dissociation rate constant will determine what effect, if any, dissociation has on the association phase of the interaction. Stated another way, if the dissociation rate constant is sufficiently small, then the association phase contains little or no information about the dissociation process (see Fig. 1B). In the present experiments, dissociation data were collected for 10,000 s at a rate of 1 Hz.

At the end of the injection of ligate, as the flow cell reverts to buffer flow, there is a period of time in which the instrument response contains a component due to the change in bulk refractive index of the two solutions (i.e., ligate versus buffer). This usually lasts for 20-30 s. In the present studies, therefore, the first 30 s after the sample has traversed the flow cell was routinely omitted from the data set prior to analysis. An example of analysis of the dissociation process, according to Eq. [11] is presented in Fig. 4. It can be seen from this figure that the data are described well by Eq. [11] with a derived apparent dissociation rate constant, k_d , of 3.98×10^{-5} s⁻¹. The residuals for this data set have a magnitude of ± 2 RU and are random. The magnitude of the residuals demonstrates the high quality data that can be obtained on the BIAcore and are a measure of goodness of fit to Eq. [11]. Since the data presented in Fig. 4 are well described by a single exponential decay (Eq. [11]), it can be concluded that the assumption that desorbed ligate does not reassociate with the layer is valid. From the modeling studies presented in Fig. 1, it may also be concluded that we would not be able to accurately derive an apparent k_d of this magnitude from the association data. demonstrating the importance of analysing the dissociation data first. Not all data sets, however, fit as well as that presented in Fig. 4. Indeed, nonrandom residuals are often observed and may reflect the mechanics of the instrument, particularly valve switching, syringe filling, pump noise, and temperature fluctuations. Even in such cases, the residuals have a magnitude of no more than ±4 RU.

Another phenomenon observed in the present study is that at high ligate concentrations (100 and 50 nM), the dissociation process is not a single exponential decay but, rather, can more accurately be described by a double exponential decay defined as

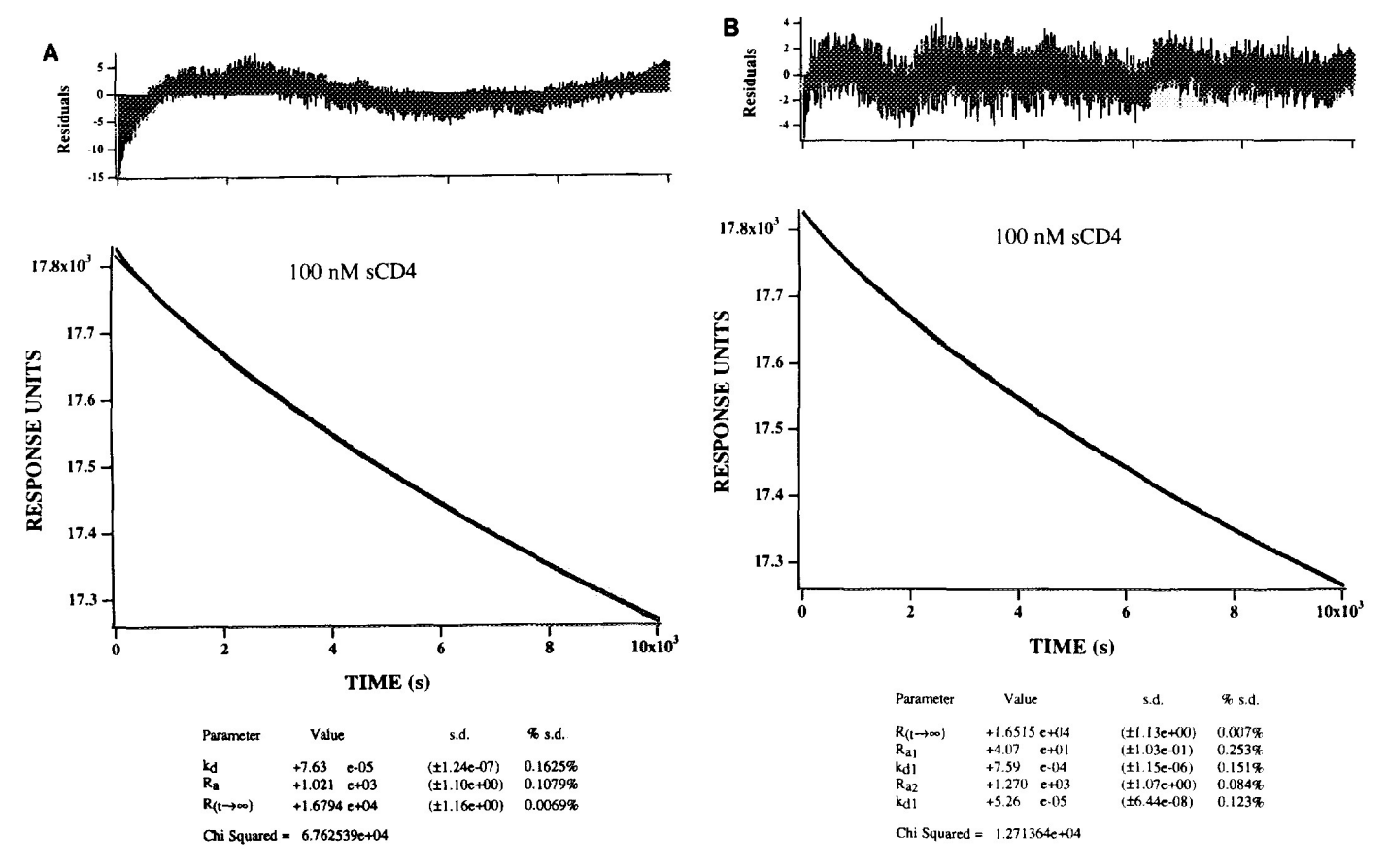


FIG. 5. Multiple dissociation of bound sCD4. The dissociation of the sCD4-L71 complex formed after injection of 100 nm sCD4 fit according to a single exponential (Eq. [11], (A) and a double exponential (Eq. [12], (B). The magnitude and associated apparent dissociation rate constants determined from the double exponential fit were: $R_{a1} = 41 \text{ RU}$, $k_{d1} = 7.6 \times 10^{-4} \text{ s}^{-1}$, $R_{a2} = 1270 \text{ RU}$, $k_{d2} = 5.26 \times 10^{-5} \text{ s}^{-1}$.

$$R_{t} = \{R_{a1}e^{-k_{d1}t} + R_{a2}e^{-k_{d2}t}\} + R_{t\to\infty}, \qquad [12]$$

where $R_{(t\to\infty)}$ is the response at infinite time and represents complete dissociation, R_{a1} is the amplitude of the dissociation process with a rate constant of k_{d1} , and R_{a2} is the amplitude of the dissociation process with a rate constant of k_{d2} . An example of this apparent multidissociation process is presented in Fig. 5. A comparison of a single exponential fit (Eq. [11]; Fig. 5A) and a double exponential fit (Eq. [12]; Fig. 5B) suggests that at least two types of complexes are formed on the sensor chip surface as one approaches saturation. A single exponential fit results in nonrandom and relatively large residuals whereas a double exponential fit results in residuals which are significantly more random and smaller in magnitude (Figs. 5A and 5B, respectively). In addition, the χ^2 value decreases significantly by inclusion of the second exponential. The magnitude and associated apparent dissociation rate constants determined for this data set according to Eq. [12] were: $R_{a1} = 41$ RU, $k_{d1} =$ $7.59 \times 10^{-4} \text{ s}^{-1}$, $R_{a2} = 1270 \text{ RU}$, and $k_{d2} = 5.26 \times 10^{-5} \text{ s}^{-1}$. It should be stressed that the second dissociation event determined for the data set presented in Fig. 5B is small, accounting for only about 3% of the total dissociation, but is reproducibly determined in such data sets and would therefore appear to be significant. In the process of immobilization the ligand randomly associates with the surface resulting in multiple orientations and, potentially, multiple affinities for the ligate. Lower affinity binding sites would become more prevalent as one approaches saturation of the surface. This is observed in the present investigation (compare Figs. 4 and 5). This phenomenon would be expected to be highly ligand dependent and suggests caution be exercised in analysis of dissociation data. An alternative explanation for the apparent double exponential dissociation process shown in Fig. 5 is that the more rapid decay is not due to weakly bound ligate, but rather to sequestered ligate diffusing out of the dextran matrix. The magnitude of this effect would also be expected to increase with increasing ligate concentration. However, it should be stressed that careful analysis of dissociation data allows one to discern such events and if necessary to characterize each process, as shown in Fig. 5.

Apparent multidissociation processes have previously been described in the analysis of BIAcore data

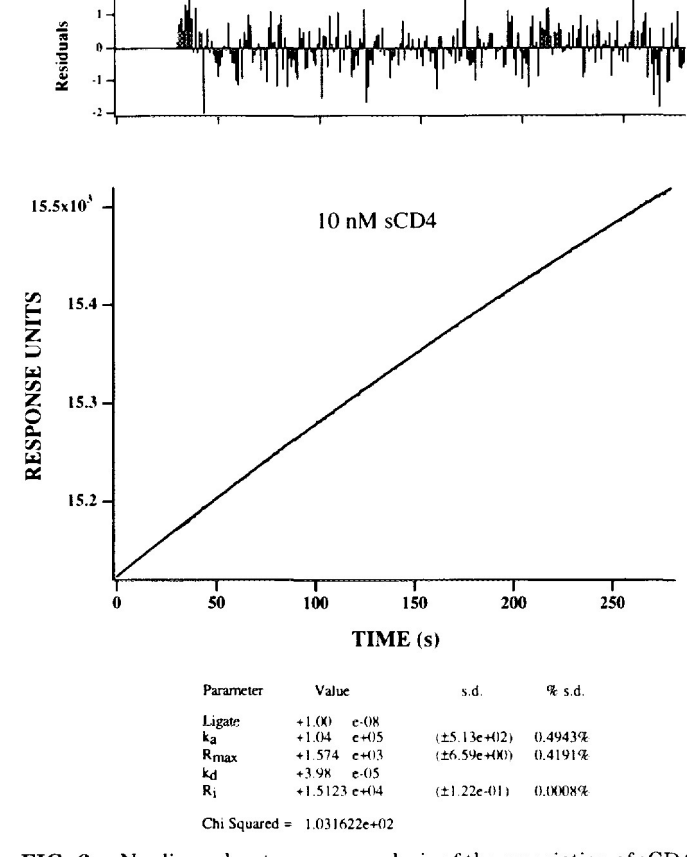


FIG. 6. Nonlinear least squares analysis of the association of sCD4 to immobilized MoAb L71. The association progress curve obtained for the binding of 10 nM sCD4 to immobilized L71 was analyzed according to Eq. [7]. The actual data points (1 per second) and the calculated line are shown on the graph. A residual plot, which is basically random with an amplitude of ± 1 RU, is also shown. The fitted parameters for this data set were: $k_a = 1.04 \times 10^5 \pm 5.13 \times 10^2 \, \mathrm{M}^{-1} \, \mathrm{s}^{-1}$, $R_{\rm max} = 1574 \pm 7$ RU, $R_{\rm i} = 15,123 \pm 0.1$ RU.

(10,12). However, these reports have used the linear transform of the rate equation, described by Eq. [9]. The nonlinear plots of $\ln(R_1/R_n)$ versus (t_n-t_1) obtained by these authors have been interpreted as multidissociation processes and the individual k_d values have been derived by arbitrarily drawing straight lines through portions of the data. Under such circumstances, use of linear least squares methods is an approximation only. There is no reason why these data should not be analyzed directly, as described here using nonlinear methods, avoiding any assumptions.

As described above for the dissociation phase, on injection of ligate there is a period lasting from 20 to 30 s, in which the response reflects not only the binding event per se but also changes in the bulk refractive index. Routinely, therefore, the association data set starts at a defined time after the injection point, in this case at t=30 s. The association phase is fit according to Eq. [7] and an example of such an analysis is presented in Fig. 6. As

can be seen, the residuals are small ($\pm 2~\mathrm{RU}; \pm 0.5\%$) and random. The apparent association rate constant calculated from the data presented in Fig. 6 was $1.04 \times 10^5~\mathrm{M}^{-1}~\mathrm{s}^{-1}$. Since the data set starts at $R_{t=30}$, one of the fitting parameters is the response at time zero, i.e., $R_{\rm i}$. According to the above discussion, an association process with an apparent dissociation rate constant of 3.98 $\times 10^{-5}~\mathrm{s}^{-1}$ contains little or no information on the dissociation process. Therefore, the data set presented in Fig. 6 was analyzed according to Eq. [7], but holding the dissociation rate constant at $3.98 \times 10^{-5}~\mathrm{s}^{-1}$ since this was accurately determined from the dissociation process.

There is at least one report (11) in the literature of apparent biphasic association data obtained on BIAcore, for the interaction of antibodies to immobilized peptides, in that dR/dt versus R plots (Eq. [4]) were nonlinear. The authors arbitrarily derived apparent k_a values from this data by drawing straight lines through the nonlinear data. As mentioned above, this analysis is only an approximation since Eq. [4] describes a single interaction between species A and B to form complexes, AB, and does not account for other interactions. We have also observed interactions on the BIAcore which can best be described by two independent interactions (O'Shannessy et al., unpublished results). Such a phenomenon can be described by Eq. [13]

$$\begin{split} R_t &= \left\{ \frac{Ck_{a1}R_{\max 1}[1 - e^{-((Ck_{a1} + k_{d1})t}]}{Ck_{a1} + k_{d1}} \\ &+ \frac{Ck_{a2}R_{\max 2}[1 - e^{-((Ck_{a2} + k_{d2})t)}]}{Ck_{a2} + k_{d2}} \right\} + R_i, \quad [13] \end{split}$$

where k_{a1} and k_{d1} are the rate constants describing one interaction with a maximal response of R_{max1} , and k_{a2}

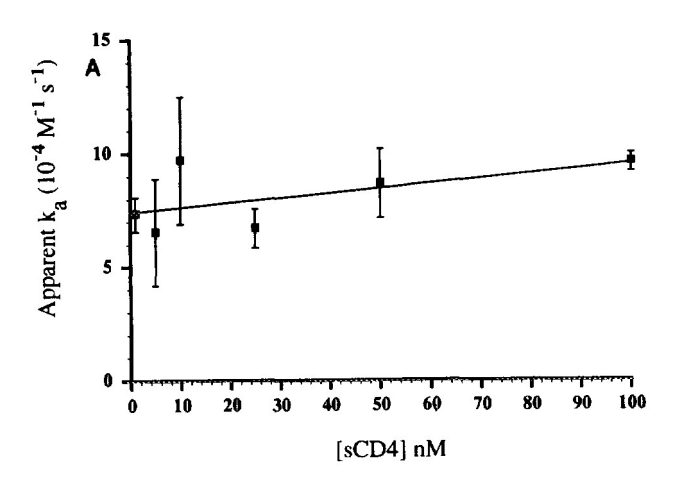
TABLE 4

Values of Apparent Rate and Equilibrium Binding Constants Determined for the Interaction of sCD4 with Immobilized MoAb L71

[sCD4] (nM)	Apparent k_a (10 ⁴ M ⁻¹ s ⁻¹)	Apparent k_d (10^{-5} s^{-1})	Apparent K_D (10^{-10} M)
100	$9.63 \pm 0.41 \ (n = 5)$	$5.39 \pm 0.79 \ (n = 5)$	5.60 ± 0.84
50	$8.69 \pm 1.52 (n = 5)$	$5.69 \pm 1.10 \ (n=4)$	6.55 ± 1.71
25	$6.70 \pm 0.86 (n = 5)$	$4.81 \pm 0.43 \ (n=4)$	7.18 ± 1.21
10	$9.69 \pm 2.80 \ (n = 5)$	$3.72 \pm 0.30 \ (n=4)$	3.84 ± 1.16
5	$6.53 \pm 2.36 \ (n = 3)$	ND^a	
1	$7.33 \pm 0.76 (n = 3)$	ND	
	$8.15 \pm 2.23 \ (n = 26)$	$4.93 \pm 1.01 \ (n = 17)$	6.05 ± 2.06

Note. Values for the apparent k_a and apparent k_d represent the mean and standard deviation of at least three independent experiments for each sCD4 concentration. The apparent k_a was determined from the association phase and the apparent k_d was determined from the dissociation phase data as described in the text.

a ND, not determined.



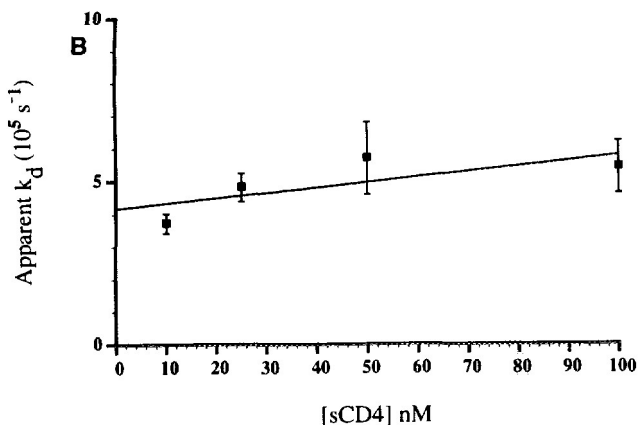


FIG. 7. Invariance of the apparent association and dissociation rate constants with ligate concentration. The apparent association rate constants, k_a , and apparent dissociation rate constants, k_d , presented in Table 1 are plotted against ligate concentration, (A and B, respectively). Both apparent rate constants are basically invariant with ligate concentration, although some scatter is observed. Linear regression analyses of these data are presented in the figure. Error bars represent the standard deviation from the mean for at least three independent experiments at each ligate concentration. Linear least squares analyses resulted in the following: (A) Apparent association rate constant, f(x) = 0.019 * x + 7.57 and $R^2 = 0.12$; (B) apparent dissociation rate constant, f(x) = 0.015 * x + 4.19 and $R^2 = 0.29$. t test analysis of these data demonstrated that the apparent association rate constant is invariable with ligate concentration ($\alpha = 0.05$, p =0.08) and that the apparent dissociation rate constant shows some dependence on ligate concentration ($\alpha = 0.05$, p = 0.02).

and k_{d2} are the rate constants describing the second interaction with a maximal response of $R_{\max 2}$. As described above, biphasic association data may also be explained by a nonspecific binding component.

While multiple association and dissociation processes can be treated approximately using linear methods, analysis of data directly using nonlinear methods is clearly an advantage.

With few exceptions, kinetic rate and equilibrium binding constants reported in the literature, as derived from BIAcore data, contain no information on the

TABLE 5
Linear Least Squares Analysis of Derivative Plots dR/dt versus R

[sCD4] nM	$k_{s}^{a}(n)$
100	$9.54 \pm 10^{-3} \pm 5.77 \times 10^{-4} (n = 5)$
50	$4.30 \pm 10^{-3} \pm 5.70 \times 10^{-4} (n = 5)$
25	$1.69 \pm 10^{-3} \pm 2.31 \times 10^{-4} (n = 5)$
10	$1.01 \pm 10^{-3} \pm 2.64 \times 10^{-4} (n = 5)$
5	$8.53 \pm 10^{-4} \pm 2.45 \times 10^{-4} (n = 3)$
1	$1.26 \pm 10^{-3} \pm 2.07 \times 10^{-3} (n = 3)$

^a Values represent the mean and standard deviation of at least three individual determinations of k_s at each concentration of sCD4. The numbers in parentheses represent the number of replicate experiments. Derivative plots (dR/dt versus R) were calculated by point to point methods.

errors associated with or the reproducibility in such determinations. This is curious since the automation of the BIAcore readily allows for multiple binding/dissociation events to be performed with limited hands-on time. This feature of the BIAcore means that generating binding data from multiple injections of ligate, at a number of concentrations, is relatively painless but allows for a thorough statistical analysis of the derived parameters. Given this, we were interested in assessing the reproducibility in the determination of the apparent ki-

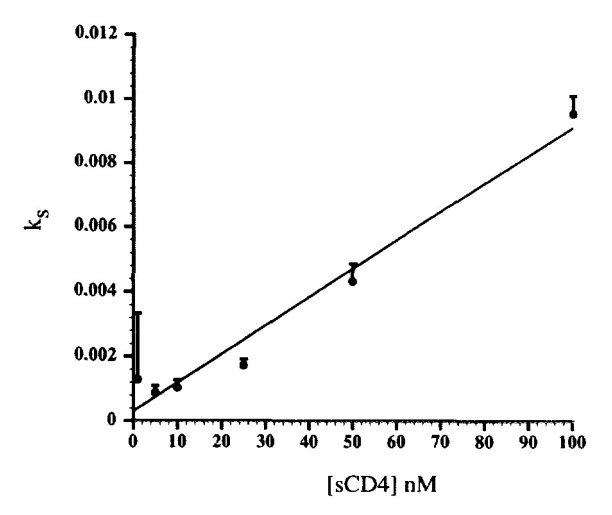


FIG. 8. Linear least squares analysis of BIAcore binding data according to Eq. [5]. A derivative analysis (point-to-point) of the association phase of each binding experiment was performed and the slope, ks, determined by linear regression analysis according to Eq. [4]. The average slope calculated for each ligate concentration was plotted versus ligate concentration according to Eq. [5]. Linear regression analysis resulted in the following parameter values: $k_a = 8.83 \pm 2.23 \times 10^4 \, \mathrm{M}^{-1} \, \mathrm{s}^{-1}$ and $k_d = 2.98 \times 10^{-4} \pm 2.04 \times 10^{-3} \, \mathrm{s}^{-1}$. Error bars represent the standard deviation from the mean for at least three independent experiments at each ligate concentration. Linear least squares analysis resulted in the following: $f(x) = 8.83 \, e - 5 * \times + 2.98 \, e - 4$ and $R^2 = 0.97$.

netic rate constants for the interaction of sCD4 with immobilized MoAb L71. Therefore, multiple samples of sCD4 at a number of concentrations were injected as described under Materials and Methods. The data were analyzed as described above (according to Eqs. [7] and [11]) and the results are presented in Table 4. A t test analysis of the concentration dependence of the apparent association and dissociation rate constants is shown in Fig. 7. The apparent association rate constant was determined to be invariant with ligate concentration, i.e., nonsignificant at $\alpha = 0.05$, actual p value = 0.08. However, the apparent dissociation rate constant was shown to be ligate concentration dependent, i.e., significant at $\alpha = 0.05$, actual p value = 0.025. It should be noted that the range of concentrations for which we have apparent dissociation rate constants is smaller than that for the apparent association rate constants. To better define the significance or otherwise of the apparent dependence of the dissociation rate constant on ligate concentration, further experiments are warranted.

As discussed above, this analysis (relationship of rate constants to ligate concentration) would not be possible using the linear least squares methods recommended by the manufacturer. From the data presented in Table 4, the apparent equilibrium binding dissociation constant, K_D , for the interaction of sCD4 with immobilized MoAb L71 was calculated to be $6.05 \pm 2.06 \times 10^{-10}$ M⁻¹.

Finally, a direct comparison was made between the linear least squares analysis recommended by the manufacturer of the BIAcore and the nonlinear least squares method described here. From plots of dR/dt versus R on the same data presented in Table 4 analyzed according to Eq. [4], slopes, ks, were calculated for each ligate injection at six concentrations. The values obtained are presented in Table 5 and displayed graphically in Fig. 8. Analysis of the ks versus C plot (Fig. 8) according to Eq. [5] resulted in the following parameter values: $k_a = 8.83$ $\pm 2.23 \times 10^4 \,\mathrm{M}^{-1} \,\mathrm{s}^{-1}$ and $k_d = 2.98 \times 10^{-4} \pm 2.04 \times 10^{-3}$ s⁻¹. Interestingly, the apparent association rate constants calculated by the nonlinear least squares and linear least squares methods are similar, cf. $8.15 \pm 2.23 \times$ 10^4 and $8.83 \pm 2.23 \times 10^4 \, \text{M}^{-1} \, \text{s}^{-1}$, respectively. Importantly, the apparent dissociation rate constant derived using the linear least squares approach is approximately sixfold greater than that determined using the nonlinear least squares approach and has a significantly higher associated error, cf. $2.98 \times 10^{-4} \pm 2.04 \times 10^{-3}$ and $4.93 \pm 1.01 \times 10^{-5}$ s⁻¹. To be fair, the manufacturer does recognize the fact that derivation of the apparent dissociation rate constant from a plot of ks versus C is not possible when the k_d is low.

From the foregoing discussion it is evident that some care must be taken in the analysis and interpretation of kinetic data generated on the BIAcore. Quantitative kinetic data can be obtained using SPR; however, the

most robust analysis of such data is obtained by analysis of the primary response using a nonlinear least squares approach. Analysis of BIAcore data according to Eqs. [7] and [11] by nonlinear least squares methods allows for the determination of the apparent kinetic rate constants, k_a and k_d , for each binding experiment and further allows for the estimation of the parameter associated errors in a way which directly reflects errors in the primary data. This is in contrast to the data analysis methods which rely on linear transformations of the primary data which result in a single value for both the association and the dissociation rate constants. This feature of nonlinear least squares analysis methods is important since it allows for the validation of the kinetic model being used to describe the process. The law of mass action requires that the rate (and equilibrium binding) constants be invariant with concentration. The data presented in Table 4 demonstrate that, for this system, this is probably the case (see Fig. 7). Since the BIAcore injection system is automated, generating multiple data sets at multiple ligate concentration is not only easy, but is also essential for a complete kinetic analysis. It should also be noted that the present kinetic models are the simplest case scenario, in that they describe the interaction of two well behaved macromolecules. This will not always be the case for interactions studied by SPR. We, and others, have observed interactions that do not fit the simple Langmurian equation but can best be described by multiple independent interactions, as described by Eq. [13] (O'Shannessy et al., unpublished results). The more complex the kinetic model, the more difficult it will be to analyze by linear least squares methods. In contrast, encoding and analyzing more complex kinetic models by nonlinear methods is straightforward. Finally, it should be reemphasized that for kinetic analyses of BIAcore data, the dissociation phase should be analyzed first to yield a relatively precise and unambiguous value of the dissociation rate constant, k_d , which can then be used to constrain the analysis of the association phase to yield a better estimate of the association rate constant, k_a .

ACKNOWLEDGMENTS

The authors acknowledge Michael Blackburn, Paul McAllister, and John Brooks for many helpful discussions.

REFERENCES

- Kronick, M. N., and Little, W. A. (1975) J. Immunol. Methods 8, 235-240.
- Raether, H. (1988) Surface Plasmons on Smooth and Rough Surfaces and on Gratings. Springer Verlag, Berlin.
- Löfås, S., and Johnsson, B. (1990) J. Chem. Soc. Chem. Commun. 1526–1528.

- Johnsson, B., Löfås, S., and Lindquist, G. (1991) Anal. Biochem. 198, 268–277.
- Sjölander, S., and Urbaniczky, C. (1991) Anal. Chem. 63, 2338– 2345.
- Stenberg, E., Persson, B., Roos, H., and Urbaniczky, C. (1991) J. Colloid Interface Sci. 143, 513-526.
- Karlsson, R., Michaelsson, A., and Mattsson, L. (1991) J. Immunol. Methods 145, 229-240.
- Chaiken, I., Rose, S., and Karlsson, R. (1991) Anal. Biochem. 201, 197-210.
- 9. Altschuh, D., Dubs, M-C., Weiss, E., Zeder-Lutz, G., and Van Regenmortel, M. H. V. (1992) Biochemistry 31, 6298-6304.
- Malmborg, A-C., Michaëlsson, A., Ohlin, M., Jansson, B., and Borrebaeck, C. A. K. (1992) Scand. J. Immunol. 35, 643-650.
- 11. Zeder-Lutz, G., Altschuh, D., Geysen, H. G., Trifilieff, E., Som-

- mermeyer, G., and Van Regenmortel, M. H. V. (1993) Mol. Immunol. 30, 145-155.
- Borrebaeck, C. A. K., Malmborg, A-C., Furebring, C., Michaëlsson, A., Ward, S., Danielsson, L., and Ohlin, M. (1992) Bio/Technology 10, 697-698.
- Brigham-Burke, M., Edwards, J. R., and O'Shannessy, D. J. (1992) Anal. Biochem. 205, 125-131.
- O'Shannessy, D. J., Brigham-Burke, M., and Peck, K. (1992) Anal. Biochem. 205, 132-136.
- Hulme, E. C., and Birdsall, N. J. M. (1992) in Receptor-Ligand Interactions. A Practical Approach (Rickwood, D., and Hames, B. D., Eds.), IRL Press, Oxford.
- 16. Wilkinson, G. N. (1961) Biochem. J. 80, 324-332.
- 17. Johnson, M. L. (1992) Anal. Biochem. 206, 215-225.
- 18. Marquardt, D. W. (1963) J. Soc. Ind. Appl. Math. 11, 431-441.